Article

Synthesis and functional assessment of a novel fatty acid probe, #-ethynyl eicosapentaenoic acid analog, to analyze the *in vivo* behavior of eicosapentaenoic acid

Tomohisa Tokunaga, Bunta Watanabe, Sho Sato, Jun Kawamoto, and Tatsuo Kurihara

Bioconjugate Chem., **Just Accepted Manuscript** • DOI: 10.1021/acs.bioconjchem.7b00235 • Publication Date (Web): 06 Jul 2017

Title

Synthesis and functional assessment of a novel fatty acid probe, ω-ethynyl eicosapentaenoic acid analog, to analyze the *in vivo* behavior of eicosapentaenoic acid

Tomohisa Tokunaga, Bunta Watanabe*, Sho Sato, Jun Kawamoto, Tatsuo Kurihara*

Institute for Chemical Research, Kyoto University, Uji, Kyoto 611-0011, Japan

*Corresponding authors

B. W.: Tel: +81-774-38-3233, Fax: +81-774-38-3229, E-mail: bunta@scl.kyoto-u.ac.jp

T. K.: Tel: +81-774-38-4710, Fax: +81-774-38-3248, E-mail: kurihara@scl.kyoto-u.ac.jp

Running Title: Novel probe to analyze eicosapentaenoic acid behavior *in vivo*

Key words: ω-3 polyunsaturated fatty acid, eicosapentaenoic acid, ω-ethynyl fatty acid probe

Abstract

Eicosapentaenoic acid (EPA) is an ω-3 polyunsaturated fatty acid that plays various beneficial roles in organisms from bacteria to humans. Although its beneficial physiological functions are well-recognized, a molecular probe that enables the monitoring of its *in vivo* behavior without abolishing its native functions has not yet been developed. Here, we designed and synthesized an ω-ethynyl EPA analog (eEPA) as a tool for analyzing the *in vivo* behavior and function of EPA. eEPA has an ω-ethynyl group tag in place of the ω-methyl group of EPA. An ethynyl group has a characteristic Raman signal and can be visualized by Raman scattering microscopy. Moreover, this group can specifically react *in situ* with azide compounds, such as those with fluorescent group, via click chemistry. In this study, we first synthesized eEPA efficiently based on the following well-known strategies. In order to introduce four C-C double bonds, a coupling reaction between terminal acetylene and propargylic halide or tosylate was employed, and then, by simultaneous and stereoselective partial hydrogenation with P-2 nickel, the triple bonds were converted to *cis* double bonds. One double bond and an ω-terminal C-C triple bond were introduced by Wittig reaction with a phosphonium salt harboring an ethynyl group. Then, we evaluated the *in vivo* function of the resulting probe by using an EPA-producing bacterium, *Shewanella livingstonensis* Ac10. This cold-adapted bacterium inducibly produces EPA at low temperatures, and the EPA-deficient mutant

(ΔEPA) shows growth retardation and abnormal morphology at low temperatures. When eEPA was exogenously supplemented to ΔEPA, eEPA was incorporated into the membrane phospholipids as an acyl chain, and the amount of eEPA was about 5% of the total fatty acids in the membrane, which is comparable to the amount of EPA in the membrane of the parent strain. Notably, by supplementation with eEPA, the growth retardation and abnormal morphology of ΔEPA were almost completely suppressed. These results indicated that eEPA mimics EPA well and is useful for analyzing the *in vivo* behavior of EPA.

Introduction

Eicosapentaenoic acid is an ω-3 polyunsaturated fatty acid with 20 carbons and 5 nonconjugated *cis* double bonds. In various organisms from bacteria to humans, EPA exists as an acyl chain of membrane phospholipids.[1,2] Phospholipids containing polyunsaturated fatty acids, such as EPA and docosahexaenoic acid (DHA), alter the physicochemical properties of membranes such as elasticity, permeability, and fluidity, and modulate the function, localization, and activity of various membrane proteins.[3,4] EPA also plays important functions as a precursor of lipid mediators. In humans, EPA and its related fatty acids, such as DHA, are converted to anti-inflammatory lipid mediators that have beneficial effects on human health.[5–7] These fatty acids play important roles in the nervous system[8] and signal transduction[9]. Moreover, supplementation of EPA and DHA possesses anti-cancer effects[10] and decrease the risk of cardiovascular disease[11]. In bacteria, EPA also plays important physiological roles. It is involved in bacterial adaptation to various conditions such as cold[12], high-hydrostatic[13], and oxidative environments[14]. *De novo* synthesis of EPA is observed in many bacteria that live in cold and high-hydrostatic environments such as the polar regions and in deep sea.[15,16] We previously revealed that *Shewanella livingstonensis* Ac10, a cold-adapted Gram-negative bacterium isolated from Antarctic seawater, inducibly produces EPA-containing phospholipids at 4 °C that support cell division, membrane organization, and membrane protein

folding at low temperatures.[12,17]

Although the physiological importance of EPA is well-recognized, information on its *in vivo* behavior, particularly in biological membranes, is very limited. This is partly due to the lack of tools for investigating EPA behavior. For example, it is currently difficult to visualize the distribution and localization of EPA *in vivo*. For this purpose, visualizable EPA analogs will be very useful. However, EPA analogs that retain the *in vivo* function of EPA and can be easily detected by standard laboratory techniques have not yet been developed. Fluorescent tags are useful for visualizing the localization of biological molecules, particularly of proteins. In the field of lipid biochemistry, fluorescent tags such as nitrobenzoxadiazole (NBD) are often used.[18,19] However, the relative bulkiness of fluorescent tags compared with the size of lipid molecules generally affects the biochemical properties of lipids. Therefore, the images obtained by using lipid molecules with fluorescent tags may not reflect the native behavior of the corresponding lipid molecules.

In this study, to overcome these problems, we designed and synthesized an ethynyl-tagged EPA analog named eEPA, which has a C-C triple bond at the omega end of EPA (Fig. 1). Because this functional group is much less bulky than fluorescent groups, eEPA may retain the *in vivo* function of EPA. The ethynyl group has a characteristic Raman signal that enables the visualization of ethynyl-tagged compounds by Raman microscopy.[20,21] In addition, the ethynyl group can specifically react with azide compounds by a 1,3-dipolar cycloaddition between azide and ethynyl groups

affording a 1,2,3-triazole ring, so called "click chemistry". Various applications of this reaction to biological science have been reported.[22] *In situ* labeling with azide-containing molecules has been widely used for visualization and affinity-tag labeling of ethynyl-tagged molecules.[23,24]

In order to evaluate the *in vivo* function of eEPA, the EPA-producing bacterium *S. livingstonensis* Ac10 and its EPA-deficient mutant (ΔEPA) are useful. We previously found that the ΔEPA strain shows growth retardation and abnormal morphology at 4 °C. Exogenous supplementation of EPA suppresses these phenotypes of ΔEPA, whereas supplementation of oleic acid does not[12]. Thus, the *in vivo* function of eEPA can be evaluated by supplementing the ΔEPA strain with eEPA. Here, we report that eEPA newly synthesized in this study retained the *in vivo* function of EPA and is therefore expected to be useful as a probe to understand the physiological functions of EPA.

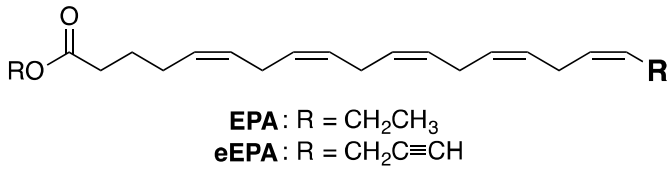

EPA: R = CH_2CH_3
eEPA: R = $CH_2C{\equiv}CH$

Figure 1. Structures of EPA and eEPA

Results and Discussion

Synthesis of eEPA

The retrosynthetic analysis of eEPA is illustrated in Scheme 1. The well-known strategy that has been successfully employed in the synthesis of PUFA analogs[25–37] was adopted in this study. The terminal ethynyl group of eEPA is introduced by a Wittig reaction of aldehyde **1**[38] using phosphonium salt **2**.[39,40] The fifth double bond between C17 and C18 is concomitantly built. The four *cis* double bonds of the key intermediate **1** are constructed by selective hydrogenation of tetrayne **3**. The skipped polyyne structure of **3** is assembled by coupling of the C1-C9 fragment **4**[41] and the C10-C17 fragment **5**. These skipped diynes come from commercially available or easily accessible materials. The convergent synthetic strategy outlined in Scheme 1 should have the advantage with respect to overall yield and number of steps over the previously reported linear synthesis of compound **1**,[38] utilizing continuous Wittig reactions. Especially, coupling reactions between terminal acetylene and propargylic halide or tosylate in carbon-carbon bond formation steps, and a stereoselective partial reduction of carbon-carbon triple bond[42] in a simultaneous hydrogenation of a resultant skipped polyyne should make the synthesis of **1** and eEPA convenient with excellent yield.

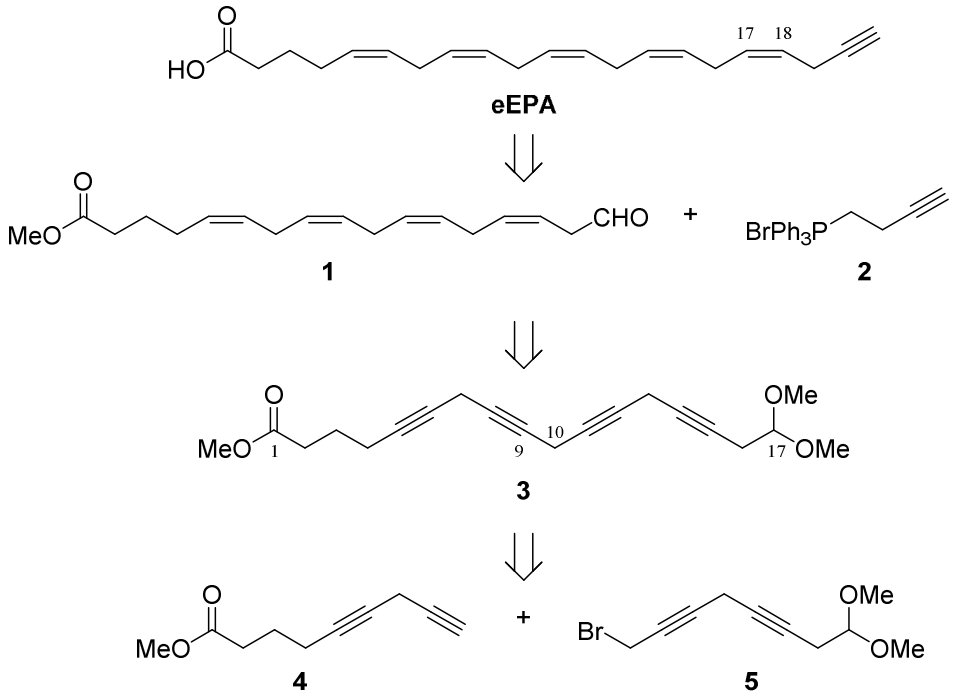

Scheme 1. Retrosynthetic analysis of eEPA

The synthesis of the C1-C9 fragment **4** is illustrated in Scheme 2. Methyl hex-5-ynoate (**6**) and 3-bromo-1-(trimethylsilyl)-1-propyne (**7**), both commercially available, were coupled by skipped diyne synthesis improved by Caruso and Spinella[43] to give diyne **8**,[44,45] without purification, with 93% yield. The trimethylsilyl group of crude **8** was removed by an $(n\text{-Bu})_4$NF/acetic acid system[46] to give the C1-C9 fragment **4**[41] with 87% yield after chromatographic purification. As mentioned in a previous study,[46] the addition of acetic acid was necessary to avoid a rearrangement of the terminal triple bond to an allene. Compound **4** was highly unstable and decomposed during storage even at –20 ºC under argon atmosphere.

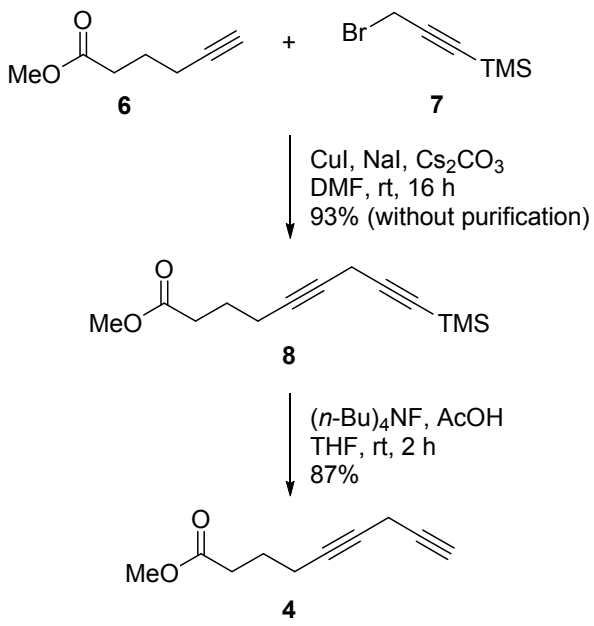

Scheme 2. Synthesis of the C1-C9 fragment 4

The synthesis of the C10-C17 fragment **5** is illustrated in Scheme 3. Monotosylate **10**,[47,48] prepared from 2-butyne-1,4-diol (**9**), was coupled with terminal acetylene **12**[49,50] to give diyne **13**, without purification, with 68% yield. Compound **12** was synthesized by the reaction between an organoaluminum reagent prepared from 3-bromo-1-propyne (**11**) and trimethyl orthoformate with 78% yield after distillation. In the previous syntheses of **12**, the organoaluminum nucleophile was generated in boiling solvents in the presence of catalytic $HgCl_2$, and the yields were 50% (in toluene)[49] to 69% (in Et_2O)[50], respectively. Lately, Gao et al. reported that various organoaluminum species could be prepared from propargylic bromides and aluminum powder in the presence of

catalytic $PbCl_2$ in tetrahydrofuran at 0 ºC.[51] By applying the improved conditions, compound **12** was prepared with 78% yield in this study The use of diethyl ether as co-solvent was found to be required for successful isolation and purification of compound **12** though it was still difficult to separate tetrahydrofuran completely. Subsequent conversion of the terminal hydroxyl group of crude **13** to a bromine atom gave the C10-C17 fragment **5** with 51% yield after chromatographic purification. Compound **5** was also highly unstable.

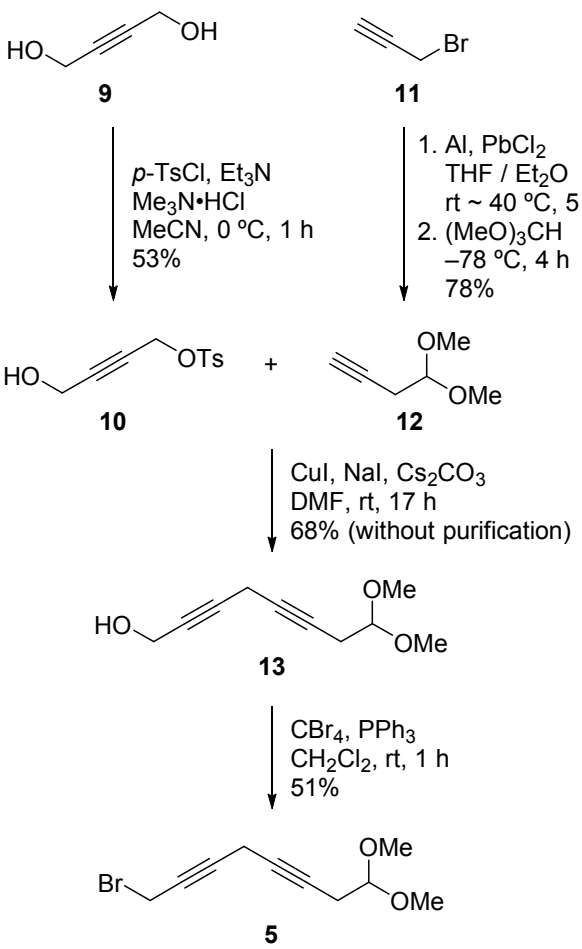

Scheme 3. Synthesis of the C10-C17 fragment 5

Now, with both the C1-C9 fragment **4** and the C10-C17 fragment **5** in hand, we coupled them under the same reaction conditions as those employed for the preparation of skipped diynes **4** and **5** to obtain tetrayne **3**, without purification, with 99% yield (Scheme 4). Compound **3** was immediately used in the subsequent step without purification since it was prone to decomposition during chromatographic purification.

Stereoselective reduction of carbon-carbon triple bonds to *cis* double bonds was extensively studied, and P-2 nickel[52] is regarded as the most reliable and efficient catalyst for partial hydrogenation of (poly)alkynic compounds to (poly)-(*Z*)-olefins.[42] Therefore, semi-hydrogenation of the four triple bonds of compound **3** to *cis* double bonds was performed with P-2 nickel, prepared from $Ni(OAc)_2 \bullet 4H_2O$ and $NaBH_4$. According to the conditions developed by Balas and co-workers,[46] the triple bonds of crude **3** were smoothly reduced as expected, and desired tetraene **14** was obtained with 65% yield after chromatographic purification. Acidic hydrolysis of the terminal dimethyl acetal of **14** gave aldehyde **1**, without purification, with 98% yield. Since aldehyde **1** is oxidized easily, it is recommended to store it at the stage of dimethyl acetal **14**. Compound **14** could be stored without decomposition for 8 months in a refrigerator under argon atmosphere. Following the Wittig reaction of crude aldehyde **1** with phosphonium ylide, prepared from phosphonium salt **2**[39,40] and *n*-BuLi, pentaene **15** was obtained with 73% after chromatographic purification. Since the

Wittig reactions between the above non-stabilized ylide and aldehydes were reported to produce *Z*-olefins[38,53,54], the geometry of the newly formed double bond between C17 and C18 of pentaene **15** was considered to be *Z*. When sodium hexamethyldisilazide was used as a base in the generation of the ylide in the reaction, the yield of the Wittig reaction was dramatically decreased. Finally, basic hydrolysis of methyl ester of **15** gave the target eEPA, without purification, with 97% yield. Since degradation of eEPA during chromatographic purification was observed, we used the product for the following experiments without further purification.

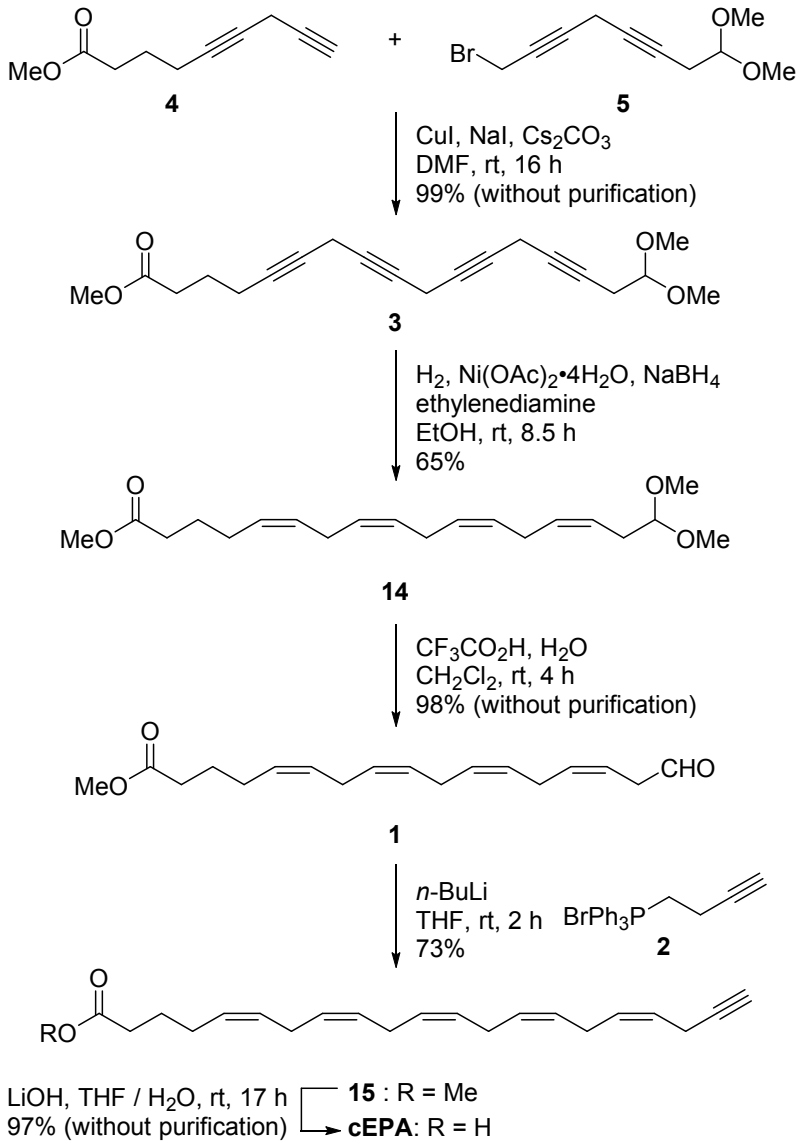

Scheme 4. Synthesis of eEPA

Bacterial uptake of exogenous eEPA

Because the ethynyl tag is a very small functional group with only two carbon atoms, and is much smaller than the fluorescent tag, biomolecules that are tagged with the ethynyl group may retain their native biological functions. To examine whether eEPA retains a specific function of EPA in living cells, we tested whether this analog is incorporated into the EPA-deficient mutant of *S. livingstonensis* Ac10 (ΔEPA) and compensates for the loss of EPA. This unique and remarkable system enables the *in vivo* functional evaluation of a particular fatty acid of interest as a substitute for EPA.

We first analyzed the phospholipid compositions of the parent cells and the ΔEPA cells grown with exogenous supplementation of EPA and eEPA at 4 °C. The phospholipids were extracted and analyzed by electrospray ionization-mass spectrometry (ESI-MS), and the mass spectra in the range of *m*/*z* 690-800, where EPA-containing phospholipids were detected, are shown in Fig. 2. EPA- and eEPA-containing phosphatidylethanolamines (PEs) and phosphatidylglycerols (PGs) detected in these samples by electrospray ionization-tandem mass spectrometry are listed in Table 1. In all these samples, phospholipids were mainly composed of PE and PG, containing various fatty acyl groups such as 16:1, 15:0, 13:0, and 16:0 (data not shown), as demonstrated previously for the parent strain and ΔEPA.[12,55] In the parent strain, 16:1-EPA-PE, 18:1-EPA-PE, and 16:1-EPA-PG were detected as

major EPA-containing phospholipids (Fig. 2A, Table 1). EPA-containing phospholipids were not found in ΔEPA (Fig. 2B). In the ΔEPA cells grown in the presence of EPA, 16:1-EPA-PE, 16:0-EPA-PE, 15:0-EPA-PE, and 16:0-EPA-PG were the major EPA-containing phospholipids (Fig. 2C, Table 1). In ΔEPA grown with exogenous eEPA supplementation, eEPA-containing PEs and PGs were detected (Fig. 2D, Table 1). Among these, 16:1-eEPA-PE, 16:0-eEPA-PE, and 15:0-eEPA-PE were more abundant than other eEPA-containing phospholipids. As shown in Fig. 2 and Table 1, the molecular weights of the eEPA-containing phospholipids are greater than the natural EPA-containing counterparts by ten *m*/*z* units because of the structural modification of eEPA from EPA [+ ethylidene group (CH) – three hydrogen atoms = 10].

Table 1. EPA- or eEPA-containing phospholipids found in *S. livingstonensis* Ac10

		WT*	ΔEPA+EPA	ΔEPA+eEPA
Acyl-chain composition	PE or PG	*m*/*z*	*m*/*z*	*m*/*z*
13:0/EPA or eEPA	PE	N.D.**	N.D.	704.7
14:0/EPA or eEPA	PE	708.5	708.4	718.5
15:0/EPA or eEPA	PE	722.7	722.4	732.7
16:1/EPA or eEPA	PE	734.6	734.6	744.6
16:0/EPA or eEPA	PE	736.6	736.5	746.5
17:1/EPA or eEPA	PE	748.6	748.6	N.D.
17:0/EPA or eEPA	PE	N.D.	750.2	N.D.
18:1/EPA or eEPA	PE	762.6	762.3	N.D.
16:1/EPA or eEPA	PG	765.6	765.6	775.4
16:0/EPA or eEPA	PG	N.D.	767.6	777.3
17:1/EPA or eEPA	PG	779.3	N.D.	N.D.
17:0/EPA or eEPA	PG	N.D.	781.5	N.D.
18:1/EPA or eEPA	PG	793.5	793.5	N.D.

* Parent strain. ** Not detected.

EPA- and eEPA-containing phospholipids were analyzed by electrospray ionization-tandem mass spectrometry in the precursor ion mode, where the precursor ions yielding $[EPA]^-$ and $[eEPA]^-$ at *m*/*z*

301 and 311, respectively, were selected.

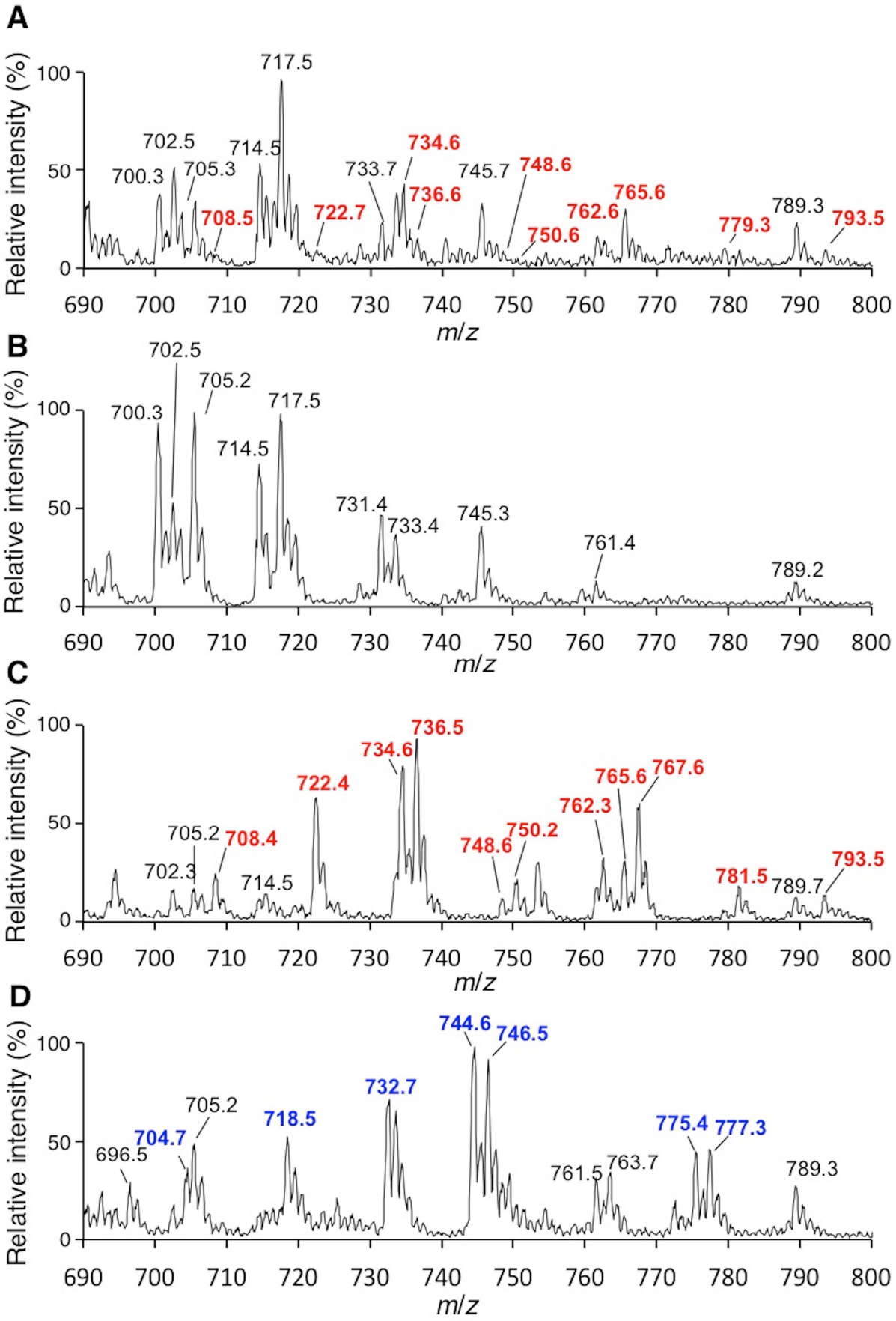
A
Relative intensity (%)
100
50
0
717.5
702.5
714.5
734.6
700.3
705.3
733.7
745.7
748.6
736.6
765.6
708.5
722.7
762.6
789.3
779.3
793.5
750.6
690 700 710 720 730 740 750 760 770 780 790 800
m/z
B
Relative intensity (%)
100
50
0
702.5
705.2
700.3
717.5
714.5
731.4
733.4
745.3
761.4
789.2
690 700 710 720 730 740 750 760 770 780 790 800
m/z
C
Relative intensity (%)
100
50
0
736.5
734.6
722.4
765.6
767.6
762.3
705.2
708.4
750.2
748.6
793.5
781.5
789.7
702.3
714.5
690 700 710 720 730 740 750 760 770 780 790 800
m/z
D
Relative intensity (%)
100
50
0
744.6
746.5
732.7
705.2
718.5
704.7
775.4
777.3
696.5
761.5
763.7
789.3
690 700 710 720 730 740 750 760 770 780 790 800
m/z

Figure 2. Phospholipid analysis of *S. livingstonensis* Ac10 grown with or without exogenous EPA/eEPA supplementation

ESI-MS analysis of the phospholipid extracts of the parent strain (A), ΔEPA (B), and ΔEPA grown with EPA (C) or eEPA (D). The spectra in the range of *m/z* 690-800 are shown. The peaks corresponding to phospholipids are indicated by their *m/z* value, and those corresponding to EPA- or eEPA-containing phospholipids are shown in red and blue, respectively.

Table 2. Acyl-chain compositions of the membrane phospholipids of *S. livingstonensis* Ac10 and the EPA-deficient mutant grown with EPA and eEPA

Acyl chain	WT*	WT + EPA	WT + eEPA	ΔEPA	ΔEPA + EPA	ΔEPA + eEPA
			(%)			
13:0	2.5 ± 0.2	3.7 ± 1.9	22.6 ± 1.5	7.5 ± 0.4	7.6 ± 0.4	27.0 ± 4.7
14:0	3.1 ± 0.2	2.3 ± 1.0	4.4 ± 0.5	2.1 ± 0.1	2.2 ± 0.0	4.5 ± 0.1
15:0	12.6 ± 0.6	17.9 ± 8.5	41.9 ± 1.6	25.1 ± 1.4	29.0 ± 1.9	37.8 ± 1.1
16:1	58.8 ± 0.7	18.3 ± 6.0	16.7 ± 3.6	50.0 ± 1.6	29.4 ± 3.6	18.8 ± 2.0
16:0	12.8 ± 1.1	14.8 ± 7.5	9.2 ± 2.0	11.2 ± 0.6	13.3 ±1.1	5.4 ± 1.5
18:1	2.3 ± 0.3	2.1 ± 1.3	6.5 ± 6.5	4.0 ± 0.3	2.4 ± 0.3	1.2 ± 0.2
EPA	8.0 ± 1.4	24.7 ± 6.2	0.4 ± 0.3	N.D. **	16.2 ± 1.2	N.D.
eEPA	N.D.	N.D.	3.3 ± 1.4	N.D.	N.D.	5.3 ± 2.7

Percentages in the total fatty acids are shown. * Parent strain. ** Not detected. Each experiment was performed three times, except for WT + EPA, with independently extracted fatty acids, and average values ± SD are shown. The experiment for WT + EPA was carried out twice.

We next analyzed the compositions of the fatty acids linked to the phospholipids. Fatty acid methyl esters were prepared from the phospholipid extracts, which do not contain free fatty acids, and quantitatively analyzed by gas chromatography-mass spectrometry (GC-MS) (Table 2). In the parent strain, the major fatty acids were 16:1, 16:0, and 15:0. The amount of EPA was 8% of the total fatty acids. In ΔEPA, the major fatty acids were 16:1, 15:0, and 16:0. In the presence of exogenous

EPA, the major fatty acids of ΔEPA were 16:1, 15:0, 16:0, and EPA. In the presence of eEPA, the major fatty acids of this strain were 15:0, 13:0, and 16:1. The reason for the increase of 13:0, a short chain-length fatty acyl group, is unclear, but this might represent a counteraction to the incorporation of eEPA, which has a longer chain length than EPA. The amount of eEPA was 5.3% of the total fatty acids and was similar to the relative amount of endogenous EPA in the parent strain grown without eEPA supplementation. These results indicate that exogenously supplemented eEPA served as the substrate for eEPA-containing phospholipid production, probably after conversion into the CoA ester, which is the substrate of 1-acyl-*sn*-glycerol-3-phosphate acyltransferase, responsible for incorporation of an acyl chain into phospholipids.[56] The structural modification of the ω-terminal of EPA to generate eEPA seems to be marginal for the enzyme in the substrate-recognition mechanism.

Biological function of eEPA

When EPA and eEPA were supplemented to the ΔEPA strain, these fatty acids were incorporated into the membrane phospholipids as their acyl chains. To test whether eEPA retains physiological functions of EPA, the growth and morphology of ΔEPA with eEPA supplementation were characterized.

Without exogenous EPA supplementation, the ΔEPA strain showed growth retardation at 4 °C due to defects in cell division (Fig. 3B). The doubling times of the parent strain and ΔEPA were

8.0 h and 13.5 h, respectively. The growth of the parent strain was not significantly affected by supplementation with EPA or eEPA (Fig. 3A). In contrast, the growth of the ΔEPA strain was improved by supplementation with EPA or eEPA (Fig. 3B). The growth rate of ΔEPA in eEPA-containing medium was similar to its growth rate in EPA-containing medium: the doubling times of ΔEPA under these conditions were 10.3 h and 9.9 h, respectively.

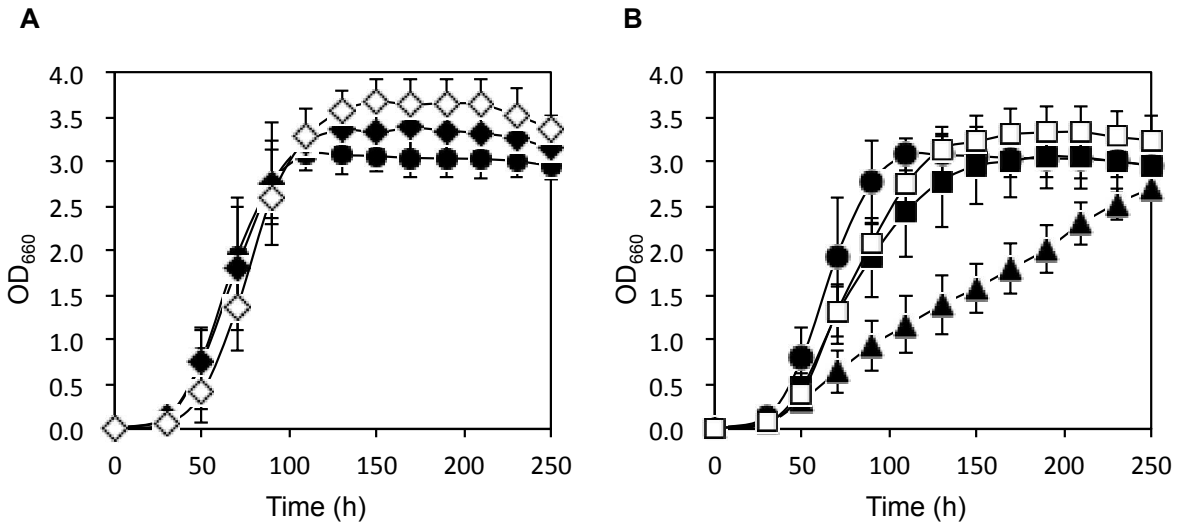

Figure 3. Growth of *S. livingstonensis* Ac10 with or without exogenous EPA/eEPA supplementation

(A) The growth curves of the parent strain in LB medium (filled circles), EPA-containing LB medium (filled diamonds), and eEPA-containing LB medium (open diamonds) at 4 °C. (B) The growth curves of ΔEPA in LB medium (filled triangles), EPA-containing LB medium (filled squares), and eEPA-containing LB medium (open squares) at 4 °C. As a control, the growth of the parent strain in LB medium (filled circle) at 4 °C is shown. The error bars indicate the standard deviation from three independent experiments.

We next analyzed the morphology of the parent strain and ΔEPA with and without supplementation of EPA or eEPA. The parent strain formed rod-shaped cells, and the cell length of about 80% of the cells was approximately 2–4 μm (Figs. 4A and E), and the average cell length was

2.9 μm. For ΔEPA without supplementation of EPA or eEPA, about 70% of cells formed filamentous cells with lengths of more than 4 μm (Fig. 4B and E). The average cell length of the mutant was 12 μm. We previously showed that the filamentous cells of ΔEPA contain multiple nucleoids, indicating that EPA is important for cell division in a step after DNA replication.[12] When EPA or eEPA was added to the medium, the cell length of ΔEPA became significantly shorter. The average length of ΔEPA under these conditions was 3.9 μm (Figs. 4C, D, and E). These data indicated that eEPA can fulfill the physiological function of EPA in this strain, at least for cell division.

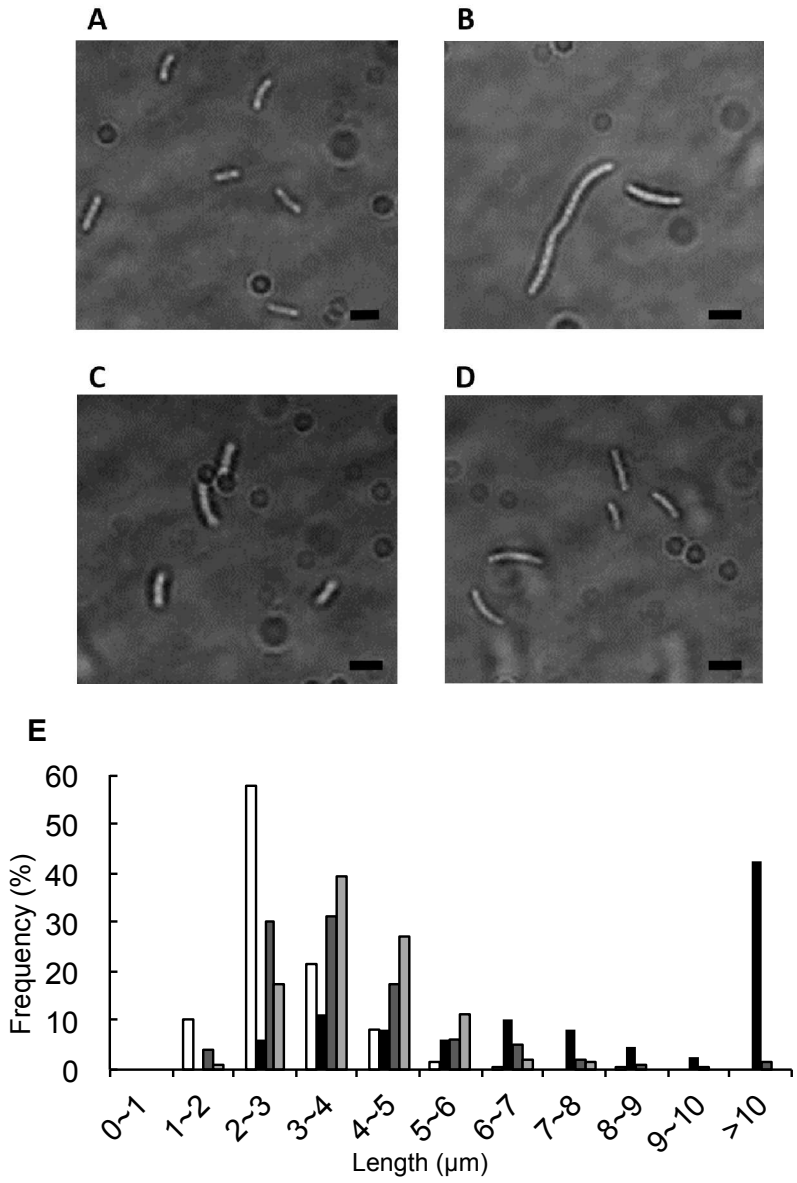

Figure 4. Morphology of *S. livingstonensis* Ac10 grown with or without exogenous EPA/eEPA supplementation

Microscopic images of the parent strain (A) and ΔEPA (B, C, and D) are shown. The cells were grown in LB medium (A and B), EPA-supplemented LB medium (C), and eEPA-supplemented LB medium (D) at 4 °C. The bar indicates 2 μm. The quantified cell size distributions of the parent strain

grown in LB medium (white) and ΔEPA grown in LB medium (black), EPA-supplemented LB medium (dark gray), and eEPA-supplemented LB medium (light gray) are shown in (E).

Significance and prospects

PUFAs such as EPA and DHA play important physiological roles in various organisms from bacteria to humans. To understand the mechanisms underlying their function, it is crucial to reveal the *in vivo* behavior of these molecules, including their subcellular localization. To analyze the subcellular localization of EPA-containing phospholipids, we previously synthesized fluorescent analogs of EPA-containing phospholipids. Although we succeeded in identifying polyunsaturated hydrocarbon chain-dependent localization of phospholipids at the cell division site of *S. livingstonensis* Ac10 using these analogs, they did not complement for the loss of EPA in this bacterium. In contrast, eEPA developed in this study suppressed the growth defects caused by the loss of EPA. Thus, our eEPA probe mimics native EPA well and is expected to provide information on the behavior of native EPA *in vivo*. Similar to other probes harboring an ethynyl group, eEPA may be visualized directly by Raman microscopy and indirectly by labeling with a fluorescent compound containing an azide group by a click chemistry reaction.[20,23,57] eEPA would also be useful for identifying EPA-containing molecules, such as EPA-modified proteins, by affinity purification[58] of eEPA-containing molecules.

It should be noted that the ethynyl group is not totally inert in a biological system under particular conditions: it was reported that the ethynyl group introduced into various steroids reacts with human liver microsomal cytochrome P450.[59] Thus it is desirable to verify that eEPA retains its original structure *in vivo* and does not disturb normal cellular functions when it is used in various organisms, although metabolic conversion of eEPA and its deleterious effects on cellular functions were not observed in the bacterial strain we used in this study.

The convergent synthetic route established in this study could synthesize compound **1**, the key intermediate for synthesis of various ω-modified EPA analogs, in half the reaction steps comparing to the previous method.[38] We believe that our approach for the synthesis of eEPA is easily applicable to the synthesis of various ω-modified EPAs such as ω-azidoEPA, ω-aminoEPA, and **ω**-deuterium-labeled EPA. These ω-modified EPAs would have various applications for studying physiological functions of EPA. For example, ω-azidoEPA and deuterium-labeled EPA would be useful for *in situ* imaging of EPA and mass spectrometric identification of EPA metabolites, respectively. Thus, it is expected that eEPA, as well as these EPA analogs, remarkably contribute to the progress of functional analysis of EPA.

Experimental Procedures

Synthesis of ω-ethynyl eicosapentaenoic acid analog, eEPA

According to the retrosynthetic analysis (Scheme 1), we synthesized eEPA as shown in Schemes 2-4. Full experimental procedures are described in the Supporting Information.

Bacterial strains and growth conditions

Strains used in this study are listed in Table 3. An EPA-producing bacterium, *S. livingstonensis* Ac10, and the EPA-deficient mutant of this strain (ΔEPA), in which one of the EPA-biosynthesis genes, *orf5,* was disrupted, were used in this study. The strains cultured on solid LB medium in the presence of 50 μg/mL rifampicin at 18 °C were aerobically precultured in 5 mL liquid LB medium (pH 7.0) for 24 h at 18 °C. The precultured cells were used as a seed culture for the following supplement assays. For the ΔEPA strain, 30 μg/mL kanamycin was added.

Table 3. Strains used in this study

Strain	Description
Shewanella livingstonensis Ac10	Parent strain of the EPA-deficient mutant[12]
ΔEPA	EPA-deficient mutant of *S. livingstonensis* Ac10, *orf5::Km*^{r} [12]

Growth and morphology in the presence of eEPA supplementation

EPA or eEPA was dissolved in ethanol (20 μL) and supplemented to 5 mL of LB liquid media at a final concentration of 0.13 mM, and *S. livingstonensis* Ac10 and its EPA-deficient mutant were grown in these media. BioPhoto recorder TVS062CA (ADVANTEC Toyo, Tokyo, Japan) was used to monitor the growth rate of the cells at 4 °C and 70 rpm. The cells were cultivated at 4 °C until the optical density at 600 nm reached about 1.0. The microscopic images of the cells were observed with a BX40F4 trinocular microscope (OLYMPUS, Tokyo, Japan) equipped with the digital microscope system, Moticam 2500 (Shimadzu Rika, Tokyo, Japan). Cell length was measured using the image-analyzing software, Image J ver. 1.6.0 (https://imagej.nih.gov/ij/).

Analysis of phospholipid composition by ESI-MS

The cells were grown in 5 mL LB medium containing 0.13 mM of EPA or eEPA at 4 °C and harvested by centrifugation when the optical density at 600 nm was approximately 1.0. After centrifugation, the collected samples were frozen in liquid nitrogen and freeze-dried by being placed in a lyophilizer, FreeZone 2.5 plus (Labconco, Kansas City, MO). Thereafter, phospholipids were extracted by the Bligh-Dyer method[60] and analyzed by ESI-MS with a triple-quadrupole Sciex API 3000 liquid chromatography-tandem mass spectrometry system (Applied Biosystems, Foster City, CA) equipped with an IonSpray ion source in the negative mode. The fatty acyl residues in each molecular species were analyzed in the precursor ion scan mode.

Analysis of fatty acyl chain composition of phospholipids by GC-MS

The cells were grown in 5 mL LB medium containing 0.13 mM EPA or eEPA at 4 °C. Phospholipids extracted from freeze-dried cells by the Bligh-Dyer method[60] were methyl-esterified with 0.5 mL of 10% HCl in methanol. Fatty acid methyl esters were extracted with 0.25 mL CH_2Cl_2 and 1 mL *n*-hexane.[61] As authentic compounds, methyl-esterified EPA and eEPA were prepared from EPA and eEPA, respectively. The methyl-esterified samples were analyzed with a Clarus 680 gas chromatograph coupled with a Clarus SQ 8 C mass spectrometer (Perkin-Elmer, Wellesley, MA) equipped with an ULBON HR-1 capillary column (Shinwa Chemical Industries, Ltd., Kyoto, Japan). Individual compounds were identified by their mass spectra. The GC-MS analysis showed that the esterification procedure did not cause significant isomerization and decomposition of authentic EPA and eEPA, indicating that these compounds are stable enough under this condition.

Acknowledgments

This work was supported in part by ICR Grants for Promoting Integrated Research from Institute for Chemical Research, Kyoto University (to JK and BW), Grant-in-Aid for Challenging Exploratory Research 26660065 (to JK), Grants-in-Aid for Scientific Research (B) from JSPS (24380047 and 15H04474 to TK), Grants from the Japan Foundation for Applied Enzymology and NAGASE

Science Technology Foundation (to TK), and a Grant-in-Aid for JSPS Fellows JP15J09839 to TT.

Some experimental measurements were carried out using the JEOL JNM-ECA600 spectrometer and the JOEL JMS-700 mass spectrometer in the Joint Usage/Research Center (JURC) at the Institute for Chemical Research, Kyoto University.

Supporting Information

Experimental procedures for eEPA synthesis.

References

(1) Calder, P. C. (2015) Marine omega-3 fatty acids and inflammatory processes: effects, mechanisms and clinical relevance. *Mol. Cell Biol. Lipids 1851*, 469–484.

(2) Yoshida, K., Hashimoto, M., Hori, R., Adachi, T., Okuyama, H., Orikasa, Y., Nagamine, T., Shimizu, S., Ueno, A., and Morita, N. (2016) Bacterial long-chain polyunsaturated fatty acids: Their biosynthetic genes, functions, and practical use. *Mar. Drugs 14*, 94, DOI: 10.3390/md14050094.

(3) Valentine, R. C., and Valentine, D. L. (2004) Omega-3 fatty acids in cellular membranes: a unified concept. *Prog. Lipid Res. 43*, 383–402.

(4) Stillwell, W., and Wassall, S. R. (2003) Docosahexaenoic acid: membrane properties of a unique fatty acid. *Chem. Phys. Lipids 126*, 1–27.

(5) Polus, A., Zapala, B., Razny, U., Gielicz, A., Kiec-Wilk, B., Malczewska-Malec, M., Sanak, M., Childs, C. E., Calder, P. C., and Dembinska-Kiec, A. (2016) Omega-3 fatty acid supplementation influences the whole blood transcriptome in women with obesity, associated with pro-resolving lipid mediator production. *Biochim. Biophys. Acta - Mol. Cell Biol. Lipids 1861*, 1746–1755.

(6) Masoodi, M., Kuda, O., Rossmeisl, M., Flachs, P., and Kopecky, J. (2015) Lipid signaling in adipose tissue: connecting inflammation & metabolism. *Biochim. Biophys. Acta - Mol. Cell Biol. Lipids*. *1851*, 503–518.

(7) Serhan, C. N., Chiang, N., and Dalli, J. (2015) The resolution code of acute inflammation: novel pro-resolving lipid mediators in resolution. *Semin. Immunol. 27*, 200–215.

(8) Bazinet, R. P., and Layé, S. (2014) Polyunsaturated fatty acids and their metabolites in brain function and disease. *Nat. Rev. Neurosci. 15*, 771–785.

(9) Gorjão, R., Azevedo-Martins, A. K., Rodrigues, H. G., Abdulkader, F., Arcisio-Miranda, M., Procopio, J., and Curi, R. (2009) Comparative effects of DHA and EPA on cell function. *Pharmacol. Ther. 122*, 56–64.

(10) Gu, Z., Shan, K., Chen, H., and Chen, Y. Q. (2015) n-3 Polyunsaturated fatty acids and their role in cancer chemoprevention. *Curr. Pharmacol. Rep. 1*, 283–294.

(11) Mozaffarian, D., and Wu, J. H. Y. (2012) (n-3) Fatty acids and cardiovascular health: are effects of EPA and DHA shared or complementary? *J. Nutr. 142*, 614S–625S.

(12) Kawamoto, J., Kurihara, T., Yamamoto, K., Nagayasu, M., Tani, Y., Mihara, H., Hosokawa, M., Baba, T., Sato, S. B., and Esaki, N. (2009) Eicosapentaenoic acid plays a beneficial role in membrane organization and cell division of a cold-adapted bacterium, *Shewanella livingstonensis* Ac10. *J. Bacteriol. 191*, 632–640.

(13) Kawamoto, J., Sato, T., Nakasone, K., Kato, C., Mihara, H., Esaki, N., and Kurihara, T. (2011) Favourable effects of eicosapentaenoic acid on the late step of the cell division in a piezophilic bacterium, *Shewanella violacea* DSS12, at high-hydrostatic pressures. *Environ. Microbiol. 13*,

2293–2298.

(14) Okuyama, H., Orikasa, Y., and Nishida, T. (2008) Significance of antioxidative functions of eicosapentaenoic and docosahexaenoic acids in marine microorganisms. *Appl. Environ. Microbiol. 74*, 570–574.

(15) Russell, N. J., and Nichols, D. S. (1999) Polyunsaturated fatty acids in marine bacteria – a dogma rewritten. *Print. Gt. Britain Microbiol. 145*, 767–779.

(16) Kato, C., and Nogi, Y. (2001) Correlation between phylogenetic structure and function: examples from deep-sea *Shewanella*. *FEMS Microbiol. Ecol. 35*, 223–230.

(17) Dai, X.-Z., Kawamoto, J., Sato, S. B., Esaki, N., and Kurihara, T. (2012) Eicosapentaenoic acid facilitates the folding of an outer membrane protein of the psychrotrophic bacterium, *Shewanella livingstonensis* Ac10. *Biochem. Biophys. Res. Commun. 425*, 363–367.

(18) Klymchenko, A. S., and Kreder, R. (2014) Fluorescent probes for lipid rafts: from model membranes to living cells. *Chem. Biol. 21*, 97–113.

(19) Amaro, M., Filipe, H. A., Prates Ramalho, J. P., Hof, M., and Loura, L. M. (2016) Fluorescence of nitrobenzoxadiazole (NBD)- labeled lipids in model membranes is connected not to lipid mobility but to probe location. *Phys. Chem. Chem. Phys. 18*, 7042–7054.

(20) Yamakoshi, H., Dodo, K., Palonpon, A., Ando, J., Fujita, K., Kawata, S., and Sodeoka, M. (2012) Alkyne-tag Raman imaging for visualization of mobile small molecules in live cells. *J. Am.*

Chem. Soc. 134, 20681–20689.

(21) Yamakoshi, H., Dodo, K., Okada, M., Ando, J., Palonpon, A., Fujita, K., Kawata, S., and Sodeoka, M. (2011) Imaging of EdU, an alkyne-tagged cell proliferation probe, by Raman microscopy. *J. Am. Chem. Soc. 133*, 6102–6105.

(22) Meldal, M., and Tomøe, C. W. (2008) Cu-catalyzed azide - alkyne cycloaddition. *Chem. Rev. 108*, 2952–3015.

(23) Luo, Z., Tikekar, R. V., and Nitin, N. (2014) Click chemistry approach for imaging intracellular and intratissue distribution of curcumin and its nanoscale carrier. *Bioconjug. Chem. 25*, 32–42.

(24) Emnett, C., Li, H., Jiang, X., Benz, A., Boggiano, J., Conyers, S., Wozniak, D. F., Zorumski, C. F., Reichert, D. E., and Mennerick, S. (2016) A clickable analogue of ketamine retains NMDA receptor activity, psychoactivity, and accumulates in neurons. *Sci. Rep. 6*, 38808, DOI: 10.1038/srep38808.

(25) Marron, B. E., Spanevello, R. A., Elisseou, M. E., Serhan, C. N., and Nicolaou, K. C. (1989) Synthesis of 19,19,20,20,20-pentadeuteriolipoxin A4 methyl ester and 19,19,20,20,20-pentadeuteriarachidonic acid. Agents for use in the quantitative detection of naturally occurring eicosanoids. *J. Org. Chem. 54*, 5522–5527.

(26) Luthria, D. L., and Sprecher, H. (1993) Synthesis of ethyl arachidonate-19,19,20,20-d_4 and ethyl dihomo-γ-linolenate-19,19,20,20-d_4. *Lipids 28*, 853–856.

(27) Dasse, O., Mahadevan, A., Han, L., Martin, B. R., Di Marzo, V., and Razdan, R. K. (2000) The synthesis of *N*-vanillyl-arachidonoyl-amide (Arvanil) and its analogs: an improved procedure for the synthesis of the key synthon methyl 14-hydroxy-(all-*cis*)-5,8,11-tetradecatrienoate. *Tetrahedron 56*, 9195–9202.

(28) Yao, F., Li, C., Vadivel, S. K., Bowman, A. L., and Makriyannis, A. (2008) Development of novel tail-modified anandamide analogs. *Bioorg. Med. Chem. Lett. 18*, 5912–5915.

(29) Ouadi, A., Habold, C., Keller, M., Bekaert, V., and Brasse, D. (2013) Synthesis of new ^{123}I-labeled free fatty acids analogues and first evaluation as potential tracers for SPECT imaging to elucidate fatty acid flux in mouse. *RSC Adv. 3*, 19040–19050.

(30) Bhar, P., Reed, D. W., Covello, P. S., and Buist, P. H. (2012) Topological study of mechanistic diversity in conjugated fatty acid biosynthesis. *Angew. Chem. Int. Ed. 51*, 6686–6690.

(31) Windsor, K., Genaro-Mattos, T. C., Kim, H.-Y. H., Liu, W., Tallman, K. A., Miyamoto, S., Korade, Z., and Porter, N. A. (2013) Probing lipid-protein adduction with alkynyl surrogates: application to Smith-Lemli-Opitz syndrome. *J. Lipid Res. 54*, 2842–2850.

(32) Lamberson, C. R., Xu, L., Muchalski, H., Montenegro-Burke, J. R., Shmanai, V. V., Bekish, A. V., McLean, J. A., Clarke, C. F., Shchepinov, M. S., and Porter, N. A. (2014) Unusual kinetic isotope effects of deuterium reinforced polyunsaturated fatty acids in tocopherol-mediated free radical chain oxidations. *J. Am. Chem. Soc. 136*, 838–841.

(33) Andreyev, A. Y., Tsui, H. S., Milne, G. L., Shmanai, V. V., Bekish, A. V., Fomich, M. A., Pham, M. N., Nong, Y., Murphy, A. N., Clarke, C. F., *et al.* (2015) Isotope-reinforced polyunsaturated fatty acids protect mitochondria from oxidative stress. *Free Radic. Biol. Med. 82*, 63–72.

(34) Niphakis, M. J., Lum, K. M., Cognetta, A. B., Correia, B. E., Ichu, T. A., Olucha, J., Brown, S. J., Kundu, S., Piscitelli, F., Rosen, H., *et al.* (2015) A global map of lipid-binding proteins and their ligandability in cells. *Cell 161*, 1668–1680.

(35) Offenbacher, A. R., Zhu, H., and Klinman, J. P. (2016) Synthesis of site-specifically ^{13}C labeled linoleic acids. *Tetrahedron Lett. 57*, 4537–4540.

(36) Golovanov, A. B., Ivanov, I. V., Groza, N. V., and Myagkova, G. I. (2015) Synthesis of rare polyunsaturated fatty acids: stearidonic and ω-3 arachidonic. *Chem. Nat. Compd. 51*, 1038–1041.

(37) Hwang, S. H., Wagner, K., Xu, J., Yang, J., Li, X., Cao, Z., Morisseau, C., Lee, K. S. S., and Hammock, B. D. (2017) Chemical synthesis and biological evaluation of ω-hydroxy polyunsaturated fatty acids. *Bioorg. Med. Chem. Lett. 27*, 620–625.

(38) Eynard, T., Poullain, D., and Vatèle, J. (1998) Synthesis of methyl (5*Z*,8*Z*,11*Z*,14*Z*,17*Z*)- and (5*Z*,8*Z*,11*Z*,14*Z*,17*E*)-[18-^{14}C] eicosapentaenoate. *J. Label. Compd. Radiopharm. 41*, 411–421.

(39) Dharanipragada, R., and Fodor, G. (1986) Search for new membrane-active substances: synthesis of tropan-3-ols with alkyl, alkenyl and alkenynyl groups at the bridgehead. *J. Chem. Soc. Trans. 1* 545–550.

(40) Haslop, A., Gee, A., Plisson, C., and Long, N. (2013) Fully automated radiosynthesis of [1-(2-[^{18}F]fluoroethyl),1*H*[1,2,3]triazole 4-ethylene] triphenylphosphonium bromide as a potential positron emission tomography tracer for imaging apoptosis. *J. Label. Compd. Radiopharm. 56*, 313–316.

(41) Kwok, P. Y., Muellner, F. W., Chen, C. K., and Fried, J. (1987) Total synthesis of 7,7-, 10,10-, and 13,13-difluoroarachidonic acids. *J. Am. Chem. Soc. 109*, 3684–3692.

(42) Oger, C., Balas, L., Durand, T., and Galano, J. M. (2013) Are alkyne reductions chemo-, regio-, and stereoselective enough to provide pure (*Z*)-olefins in polyfunctionalized bioactive molecules? *Chem. Rev. 113*, 1313–1350.

(43) Caruso, T., and Spinella, A. (2003) Cs_2CO_3 promoted coupling reactions for the preparation of skipped diynes. *Tetrahedron 59*, 7787–7790.

(44) Chemin, D., Gueugnot, S., and Linstrumelle, G. (1992) An efficient stereocontrolled synthesis of 12(*R*)-HETE and 12(*S*)-HETE. *Tetrahedron 48*, 4369–4318.

(45) Mohamed, Y. M. A., and Hansen, T. V. (2011) Synthesis of methyl (5*Z*,8*Z*,10*E*,12*E*,14*Z*)-eicosapentaenoate. *Tetrahedron Lett. 52*, 1057–1059.

(46) Balas, L., Durand, T., Saha, S., Johnson, I., and Mukhopadhyay, S. (2009) Total synthesis of photoactivatable or fluorescent anandamide probes: novel bioactive compounds with angiogenic activity. *J. Med. Chem. 52*, 1005–1017.

(47) Dumez, E., Faure, R., and Dulcère, J.-P. (2001) Diastereoselective access to 3-nitro-4-vinylidenetetrahydrofurans and 3-nitro-4-vinylidenetetrahydropyrans and their conversion into 3,6-dihydro-1,2-oxazines by reverse cope elimination of hydroxylamine precursors. *Eur. J. Org. Chem. 2001*, 2577–2588.

(48) Martin, D. B. C., Nguyen, L. Q., and Vanderwal, C. D. (2012) Syntheses of strychnine, norfluorocurarine, dehydrodesacetylretuline, and valparicine enabled by intramolecular cycloadditions of Zincke aldehydes. *J. Org. Chem. 77*, 17–46.

(49) Jung, M. E., and Gardiner, J. M. (1994) Asymmetric synthesis of carbohydrates: synthesis of 2-deoxy-D-and 2-deoxy-L-xylofuranosides from a simple achiral precursor. *Tetrahedron Lett. 35*, 6755–6758.

(50) Shang, S., Iwadare, H., Macks, D. E., Ambrosini, L. M., and Tan, D. S. (2007) A unified synthetic approach to polyketides having both skeletal and stereochemical diversity. *Org. Lett. 9*, 1895–1898.

(51) Guo, L. N., Gao, H., Mayer, P., and Knochel, P. (2010) Preparation of organoaluminum reagents from propargylic bromides and aluminum activated by $PbCl_2$ and their regio- and diastereoselective addition to carbonyl derivatives. *Chem. Eur. J. 16*, 9829–9834.

(52) Brown, J. A., and Ahuja, V. K. (1973) Catalytic hydrogenation, VI. The reaction of sodium borohydride with nickel salts in ethanol solution. P-2 nickel, a highly convenient, new, selective

hydrogenation catalyst with great sensitivity to substrate structure. *J. Org. Chem. 38*, 2226–2230.

(53) Perl, N. R., Ide, N. D., Prajapati, S., Perfect, H. H., Durón, S. G., and Gin, D. Y. (2010) Annulation of thioimidates and vinyl carbodiimides to prepare 2-aminopyrimidines, competent nucleophiles for intramolecular alkyne hydroamination. Synthesis of (-)-crambidine. *J. Am. Chem. Soc. 132*, 1802–1803.

(54) Kobayashi, Y., Morita, M., Ogawa, N., Kondo, D., and Tojo, T. (2016) Asymmetric synthesis of 12-hydroxyheptadecatrienoic acid and its 5,6-dihydro- and 14,15-dehydro-derivatives. *Org. Biomol. Chem. 14*, 10667–10673.

(55) Sato, S., Kurihara, T., Kawamoto, J., Hosokawa, M., Sato, S. B., and Esaki, N. (2008) Cold adaptation of eicosapentaenoic acid-less mutant of *Shewanella livingstonensis* Ac10 involving uptake and remodeling of synthetic phospholipids containing various polyunsaturated fatty acids. *Extremophiles 12*, 753–761.

(56) Cho, H.-N., Kasai, W., Kawamoto, J., Esaki, N., and Kurihara, T. (2012) Characterization of 1-acyl-*sn*-glycerol-3-phosphate acyltransferase from a polyunsaturated fatty acid-producing bacterium, *Shewanella livingstonensis* Ac10. *Trace Nutr. Res. 29*, 92–99.

(57) Hong, V., Steinmetz, N. F., Manchester, M., and Finn, M. G. (2010) Labeling live cells by copper-catalyzed alkyne-azide click chemistry. *Bioconjug. Chem. 21*, 1912–1916.

(58) Zhou, B., An, M., Freeman, M. R., and Yang, W. (2014) Technologies and challenges in

proteomic analysis of protein *S*-acylation. *J. Proteomics Bioinform. 7*, 256–263.

(59) Guengerich, F. P. (1990) Mechanism-based inactivation of human liver microsomal cytochrome P-450 IIIA4 by gestodene. *Chem. Res. Toxicol. 3*, 363–371.

(60) Bligh, E. G., and Dyer, W. (1959) A rapid method of total lipid extraction and purification. *Can. J. Biochem. Physiol. 37*, 912–917.

(61) Ito, T., Gong, C., Kawamoto, J., and Kurihara, T. (2016) Development of a versatile method for targeted gene deletion and insertion by using the *pyrF* gene in the psychrotrophic bacterium, *Shewanella livingstonensis* Ac10. *J. Biosci. Bioeng. 122*, 645–651.

Table of Contents Graphic